Chapter 2
Tongue Images Acquisition System Design

Abstract In order to improve the quality and consistency of tongue images acquired by current imaging devices, this research aims to develop a novel imaging system which can faithfully and precisely record human tongue information for medical analysis. A thorough demand analysis is first conducted in this chapter in order to summarize requirements for rendering all possible medical clues, i.e., color, texture, and geometric features. Then a series of system design criteria are illustrated, and following from them three hardware modules of the imaging system, including the illuminant, lighting path, and imaging camera, are optimally proposed. Moreover, one built-in software module, the color correction process, is also provided to compensate for color variations caused by system components. Finally, several important performance indicators, including illumination uniformity, system reproducibility, and accuracy, were tested. Experimental results showed that captured images were of high quality and remained stable when acquisitions are repeated. The largest color difference between the images acquired at different times was 1.6532, which is hardly distinguishable by human observation. Compared to existing devices, the proposed system could provide a much more accurate and stable solution for tongue image acquisition. Furthermore, this developed imaging system has been evaluated by doctors of Traditional Chinese Medicine for almost 3 years and over 9000 tongue images have been collected. Analysis results based on these data also validate the effectiveness of the proposed system.

2.1 Introduction

Visual inspection of the human tongue offers a simple, immediate, inexpensive, and noninvasive solution for various medical applications. However, since the tongue is traditionally observed by the human eye rather than recorded by digital instruments, it is difficult or even impossible to quantitatively store and process tongue images. This intrinsic drawback has seriously impeded the standardization and quantification of tongue inspection for medical applications. Building a high quality and consistent tongue imaging system is essential to promote the modernization and popularization of computerized tongue diagnosis. By the aid of such an imaging

D. Zhang et al., *Tongue Image Analysis*, DOI 10.1007/978-981-10-2167-1_2

system, further applications could also be developed, such as digital data storage, computer-aided image analysis, and data transmission via the Internet for telemedicine applications.

With the development of digital imaging technology, the use of a digital camera in tongue inspection has been investigated for several years. Ten imaging systems have been implemented and a detailed introduction of these devices is presented in Table 2.1. However, based on much literature, there are two main problems in the current research. First, these systems were designed without following any common criteria, and hence there was no guidance for the design of system components. Thus several obvious design deficiencies can be noted and their recorded images may be of inferior quality. For instance, (Jang et al., 2002; Wong & Huang, 2001; Zhang, Wang, Zhang, Pang, & Huang, 2005) utilized halogen tungsten lamps whose color temperature is too low to render color in high fidelity, and thus their produced images are reddish-biased which lead to inaccurate analysis results. Also, as Fig. 2.1 shows, (Cai, 2002; Chiu, 2000; Pang, Zhang, Li, & Wang, 2004; Jiang, Chen, & Zhang, 2000) the images were captured in a public office environment, which caused the acquired images to be easily affected by the environmental illumination. Furthermore, several systems (He, Liu, & Shen, 2007; Jang et al., 2002; Wong & Huang, 2001) did not involve a color correction procedure which corrects color variations caused by system components, and thus their produced images may be unstable and unreliable. In addition, most of these systems utilized a digital still camera which suffers from blurred motion or inconsistent exposure, and the involvement of a PC for image taking would make this system inconvenient for portable data acquisition. Second, another problem in the current research is that all these devices have not been systematically tested for their accuracy and consistency. From Table 2.1, it can be seen that these developed systems substantially disagree with one another in terms of their system compositions. Various types of imaging cameras and lighting sources with diverse imaging characteristics were utilized. Therefore, the quality of the obtained tongue images considerably varies. This kind of inconsistent image representation makes images capture by different devices incompatible and noninterchangeable. Developed algorithms and obtained results based on these captured images would be unstable and inconvincible. Hence, a comprehensive test of the designed system to ensure their accuracy and stability is necessary. In view of this situation, it is crucial and urgent to develop a high quality and consistent tongue imaging system for computerized tongue image analysis.

This chapter aims to solve problems in the current research of tongue image acquisition, i.e., defective quality and inconsistent image rendering, and thus to propose a new tongue imaging system which can acquire images of high quality and great consistency. First, because the main reason which leads to the present trouble is the lack of design guidance which illustrates critical requirements to ensure accurate and consistent image acquisition, an in-depth requirement analysis of tongue imaging system design is conducted, and then a series of fundamental criteria are established to satisfy these requirements to accurately and consistently extract all possible medical clues, including color, texture, and geometric features for medical analysis. Thereafter, each module of the system, including the illuminant, lighting path, imaging camera, and post-processed color correction procedure,

Table 2.1 Summary of existing tongue image acquisition devices

Year	Illumination	Imaging camera	Color correction	System test	References
2000	Two fluorescent lamps installed in office environment (5400 K)	440 × 400 pixels in a 2/3 CCD camera	Printed color card	No	Chiu (2000)
2000	Daylight-type compact fluorescent lamp (5400 K, Kaiser RB 5000)	Nikon E1, 1280 × 1000	Gray card	No	Jiang et al. (2000)
2001	Halogen tungsten lamps (3100 K)	Olympus DSC camera	N/A	No	Wong and Huang (2001)
2002	Office illumination	Commercial digital still camera, 640 × 480	Munsell Colorchecker	No	Cai (2002)
2002	Optical fiber source (250 W halogen lamp, 4000 K)	Watec WAT-202D CCD camera, 768 × 494	N/A	No	Jang et al. (2002)
2002	OSRAM L18/72-965 fluorescent lamp (6500 K)	Kodak DC 260, 1536 × 1024	Printed color card	No	Wei et al. (2002)
2004	Four standard light sources installed in dark chest (5000 K)	Canon G5, 1024 × 768	Printed color card	No	Wang, Zhou, Yang, and Xu (2004)
2005	Two 70 W cold-light type halogen lamps (4800 K)	Sony 900E video camera, 720 × 576	Printed color card	No	Zhang et al. (2005)
2007	PHILIPS YH22 circular fluorescent lamps (7200 K)	DH-HV3103 CMOS camera, 2048 × 1536	N/A	No	He et al. (2007)
2007–2010	KOHLER illumination light source (wavelength ranges 403–865 nm)	Hitachi KP-F120 CCD camera	N/A	No	Du, Liu, Li, Yan, and Tang, (2007), Li, Wang, Liu, and Sun (2010), Li and Liu (2009), Li, Wang, Liu, Sun, and Liu (2010)

Reprinted from Wang and Zhang (2013b), with permission from Elsevier

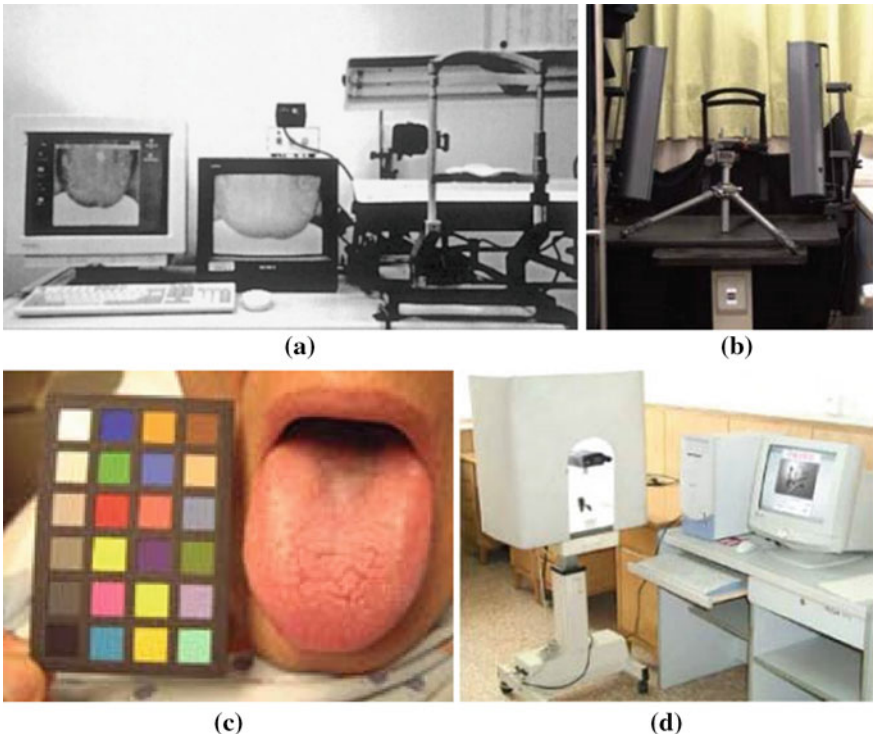

Fig. 2.1 Appearance of existing tongue imaging systems **a** Chiu's system (Chiu, 2000), **b** Jiang's system (Jiang et al., 2000), **c** Cai's device (Cai, 2002), and **d** Wei's imaging device (Wei et al., 2002). All these systems have design deficiencies which lead to production of images with poor quality. Reprinted from Wang and Zhang (2013b), with permission from Elsevier

is optimally designed. Finally, several critical system performance indicators, including illumination uniformity, system reproducibility, and accuracy, are tested to verify the validity of the proposed system.

The remainder of this chapter is organized as follows. Section 2.1 describes the system framework and corresponding requirements for each module to achieve superior quality and consistent tongue image acquisition. The detailed introduction about how each module of the system is optimally implemented is presented in Sect. 2.2. In Sect. 2.3, we conduct a performance evaluation of the proposed system. Finally, the chapter is concluded in Sect. 2.4.

2.2 System Framework and Requirement Analysis

In this section, the framework of the proposed tongue imaging system is introduced and the four principal modules of this system are presented. Then, in order to make sure the human tongue body is accurately and consistently recorded for medical

analysis, a thorough requirement analysis is provided to illustrate design criteria for each module of the system.

2.2.1 System Framework

In a typical imaging system, besides the object itself, the other two important factors are illumination and the digital detector. Illumination can be further considered as two independent parts, one is the illuminant which is mainly what types of lighting source should be selected, while the other one is the lighting path which is the design of the optical path and environmental condition. In addition to the above three hardware modules, the color correction process which compensates for variations caused by the system components and to render color images into device-independent color space, is also included in our system as a built-in software module.

Figure 2.2 presents the flowchart of the proposed tongue imaging system. There are four modules in the system: the illuminant, lighting path, imaging camera, and color correction process, are essential for accurate and consistent image acquisition. Illuminated by two carefully selected fluorescent lamps (OSRAM L8W-954), the human tongue is recorded in video file by a 3-CCD video camera (Sony DXC 390P) with a fixed-focal lens (Computer, M0814-MP). Then, the tongue image is extracted and saved by a frame grabber (Euresys Picolo Pro 2). Then, these captured tongue images are sent to the built-in embedded system for the color correction process. In our device, an embedded single board computer (Intel i5 Q1500 2.20 GHz, 2 GB RAM) is used because of its high performance, low power cost, and abundant expansion interfaces. This single board computer was assembled

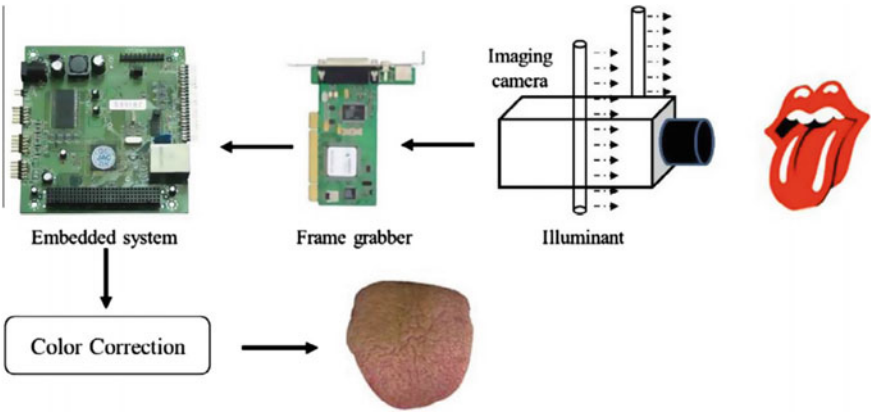

Fig. 2.2 Framework of the proposed tongue imaging system. Reprinted from Wang and Zhang (2013b), with permission from Elsevier

inside the tongue device, and the Windows XP system was installed. Hence, our developed color correction and other related tongue image analysis program could be developed and run on the Windows platform.

The four most critical modules in this system are the illuminant (L), imaging camera (C), lighting path (E), and built-in color correction algorithm (D). If the tongue imaging system is considered as a signal-transfer system which transfers the original tongue signal (denoted by T) to a digital image signal (denoted by I), then characteristics of the four modules can be viewed as significant parameters in the system's transfer function. The relationship between the input signal and output tongue image signal can be formulated as

$$I = T * f(L, C, E, D) \tag{2.1}$$

In this formula, f (L, C, E, D) is the transfer function of the proposed tongue imaging system. L, C, E, and D denote characteristics of four modules which need to be optimized. In order to achieve high quality and consistent tongue image acquisition, these four parameters need to be optimally designed, which is presented in Sect. 2.4.

2.2.2 Requirement Analysis

In TCM the tongue has been considered an essential health index of the human body for a long time, and various types of tongue features have been utilized for medical diagnosis. In order to develop the most suitable and the best quality tongue imaging system for medical analysis, we first summarize all possible features and explore their corresponding requirements on imaging system, and then the system can be easily designed.

According to the principle of tongue diagnosis (Li, 2011; Maciocia, 1987, 2013), three types of features are commonly utilized for medical analysis. The first and most essential one is the tongue color. Figure 2.3 shows four tongue images which present different colors. In the first image the tongue's proper color is red, and the remaining three tongue coating colors are yellow, white, and black respectively. These typical color types are highly correlated to various health statuses of the human body. In order to achieve accurate tongue image analysis, an imaging

Fig. 2.3 Typical tongue image samples with diverse chromatic characteristics. The main color components of these four images are red, yellow, white, and black from left to right respectively. Reprinted from Wang and Zhang (2013b), with permission from Elsevier

Fig. 2.4 Typical tongue image samples with different texture styles. Reprinted from Wang and Zhang (2013b), with permission from Elsevier

camera needs to faithfully render all types of colors, and thus to record abundant color information of high quality and fidelity in order to distinguish different kinds of diseases. Furthermore, acquired color features should be kept stable among different acquisition sessions in order to achieve a consistent performance.

Besides the color feature, texture features are also frequently utilized for medical diagnosis. Figure 2.4 shows images with typical texture features which include tongue fissure, crack, and local substance. In Fig. 2.4, the first two are images with a tongue fissure. The third one is a tongue crack and the last one is an image with local substance (red point). Different texture styles convey various pathological information of internal organs, for example a red point is usually found on the tongue of a subject with appendicitis. These texture features have distinct spatial dimensions. For example, a tongue crack is often larger than a tongue fissure, and the red point is usually the smallest texture feature style. The fundamental requirement for texture recording is to ensure adequate resolution for distinguishing the smallest texture feature style. Moreover, the obtained texture features should be clear and stable enough, and several deficiencies including motion blur and inconsistent exposure should be avoided.

Another vital feature for tongue diagnosis is the geometric feature (Huang, Wu, Zhang, & Li, 2010). As shown in Fig. 2.5, the tongue length, width, and other

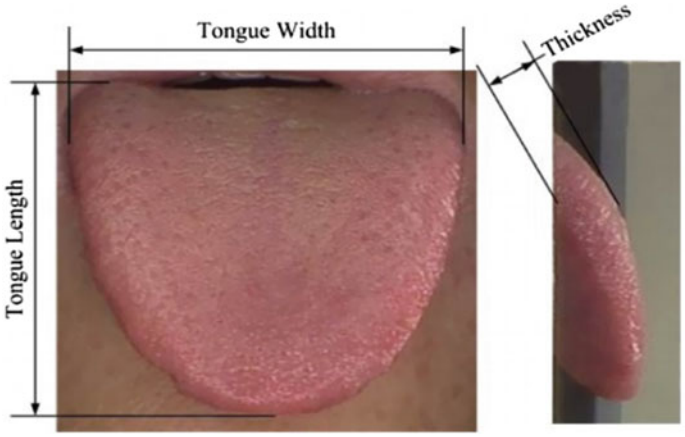

Fig. 2.5 Commonly used tongue geometric features. Reprinted from Wang and Zhang (2013b), with permission from Elsevier

geometric indexes which describe the tongue shape are crucial for diagnosis of several specific diseases (Maciocia, 2013). Also, other kinds of geometric features, including the width–length ratio, area of the tongue body, and inscribed-circle diameter, are frequently used for medical analysis. Moreover, the thickness of the tongue body is similarly found to be useful to reveal pathological changes of internal organs. Thereby, in our proposed system, in addition to a frontal image, a side view image is also captured.

In order to accurately extract all the above tongue features, we link each request with the corresponding system modules in order to establish criteria for the design of the imaging system. For instance, in order to stably and accurately capture tongue color, an illuminant with a high color rending index should be selected. Also, the color correction procedure should be involved to correct variations caused by system components. Table 2.2 provides a summary of all requirements and possible solutions to fulfill them. Section 2.3 will describe how to design the system in order to meet all these requirements.

Table 2.2 Requirement analysis for tongue imaging system design in order to ensure high-quality and consistent acquisition

Image features	Requirement	Problem domain	Possible solution
Color	High quality and fidelity	Illuminant Imaging camera Lighting path	Select illuminant with: high color rendering index and, full spectral radiation, white color Involve more CCDs (a three-CCD camera is better than a single-CCD camera) Utilize an industrial camera rather than a commercial camera to avoid built-in color enhancement Realized uniform illumination on the capture plane Utilize the lighting and viewing geometry recommended by CIE Capture images in a dark chest, not in open-air
Texture	High stability High clarity	Color correction Imaging camera	Design a color correction algorithm to calibrate acquired tongue images Have enough resolution to distinguish the smallest texture features Avoid motion blur
Geometry	Thickness feature involved	Viewing environment and optical path	Design the imaging path to acquire tongue thickness information
	User-friendly collection	Ease-of-use design	Small size Clean and safe collection Ergonomic interface design

Reprinted from Wang and Zhang (2013b), with permission from Elsevier

2.3 Optimal System Design

Based on the aforementioned proposed framework of a tongue imaging system, this section will design each module to meet all the requirements in order to ensure accurate and consistent image acquisition.

2.3.1 Illuminant

The illuminant plays an indispensable role in achieving high performance of tongue image acquisition. If the illuminant changes or has a minor variation, the color perceptions of the same tongue body may differ. Generally, there are two essential parameters needed to select the most suitable illuminant. One is the color rendering index, and the other one is the color temperature.

The color rendering index, or CRI, of a light source describes its capability to accurately render the colors of perceived objects. This index is usually expressed as a number ranging from 0 to 100, where 100 represents the perfect illuminant which can accurately render all colors. As a general rule, the higher the light source's CRI number, the better the lamp will make things appear. This index is the only internationally agreed indicator of the relative color rendering ability which provides some guidance for illuminant assessment. In a tongue imaging system, since the objective is to render tongue colors as accurately as possible, an illuminant with a high color rendering index is needed. According to the international standard on viewing conditions in graphic technology and photography (ISO, 2009), the CRI number of the selected illuminant should be larger than 90 for precise color measurement. Therefore, among all kinds of illuminants, we chose the illuminant which has the largest CRI number (bigger than 90) for tongue imaging.

Another notable characteristic of an illuminant is color temperature. It defines the color appearance of the illuminant, such as its whiteness, yellowness, or blueness. Color temperature is conventionally denoted in the unit of absolute temperature, Kelvin (K). Usually, an illuminant with color temperatures over 7000 K appears bluish, while a low color temperature (2700–3000 K) is yellowish. If an illuminant itself has some color, it cannot accurately render tongue images. Figure 2.6 shows several tongue images which were captured by four illuminants with a distinctive color temperature: an incandescent bulb (3000 K), metal halide lamp (4200 K), fluorescent lamp (5000 K), and fluorescent lamp (6500 K). It should be noted that in the first two images (a and b), the red and yellow component are slightly enhanced, while the last image is somewhat bluish biased. Only Fig. 2.6c shows a balanced color tone to TCM professionals. Thereby, based on the observation of this experiment, an illuminant with a color temperature around 5000 K is suitable for tongue color measurement. Also, according to TCM diagnostic practice, the best illuminant for tongue inspection is sunshine in an open area at 9 a.m. whose color temperature is around 5000–6000 K. This is also in accord

Fig. 2.6 Images of the same tongue body captured under different lighting source. **a** Incandescent bulb (3000 K), **b** metal halide lamp (4200 K), **c** fluorescent lamp (5000 K), and fluorescent lamp (6500 K). Reprinted from Wang and Zhang (2013b), with permission from Elsevier

with the suggestions of ISO3664:2009 (ISO, 2009), in which an illuminant with a color temperature around 5000–6000 K is recommended for unbiased color inspection and measurement. Therefore, based on our experimental findings and ISO standards, an illuminant with a color temperature between 5000 and 6000 K was chosen.

Based on the above analysis of the selection of the most suitable illuminant, and moreover, in order to reduce the dimensions of the imaging device, an OSRAM fluorescent lamp (L8W-954) was finally chosen after comparing a number of products manufactured by lighting companies (OSRAM, Philips, and GE lighting). It is a type of fluorescent lamp which has an extremely strong color rendering ability. Both its color rendering index (P90) and color temperature (5400 K) meet our above criteria (Table 2.2) to guarantee highly accurate tongue color rendering. Moreover, this illuminant is the smallest one (288 mm in length) among all illuminants which have such a high color rendering capability. This small dimension makes it possible to reduce the total size of the imaging device.

2.3.2 Lighting Condition

In addition to selecting the most suitable illuminant for tongue imaging, a lighting path, which includes the optical path and environmental illumination, also plays an essential role in the imaging process.

For the optical path design for precise color measurement, one important concern is how to position the illuminant and imaging camera to achieve a high quality of measurement. CIE (Commission International de L'Eclairage) has provided four standard options for illuminating and viewing geometry (as Fig. 2.7 shows) in reflectance color measurement. These standard illuminating and viewing conditions provide essential geometrical rules to position the illuminant and imaging detector. For example, Fig. 2.7a shows the 45°/0° geometry which recommend illuminating at 45° and viewing at 0°. By following this, reflections caused by a moist tongue surface which significantly affects the color perception of tongue images can be greatly reduced. Thereby, high-quality tongue image acquisition can be assured.

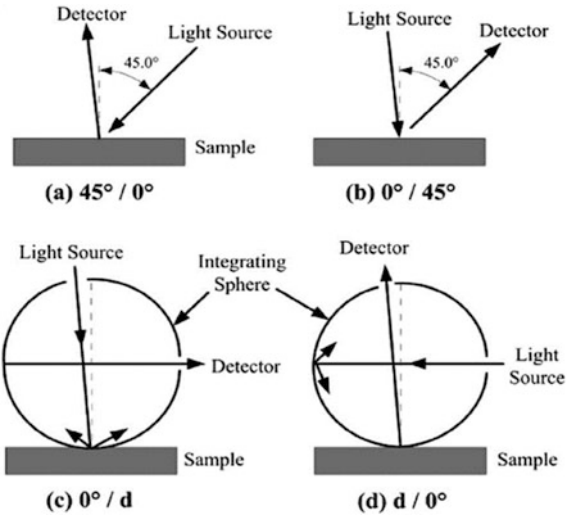

Fig. 2.7 CIE standard illuminating and viewing conditions for precise color measurement. There are four kinds of viewing and illuminating geometries which are recommended by CIE to avoid reflected light. Reprinted from Wang and Zhang (2013b), with permission from Elsevier

Based on the above standard geometry of illuminating and viewing, the optical path proposed in this work is shown in Fig. 2.8. The video camera is placed at the center. The positioning of the illuminant and imaging video camera follows the standard 45°/0° geometry to avoid reflection caused by a moist tongue surface. Moreover, in order to achieve uniform distribution of illumination on the acquisition plane, two lamps are symmetrically placed on either side of the central video camera. In addition, this system is also designed to simultaneously capture the front-view image and the side-view image. A plane mirror is placed beside the acquisition plane to reflect the side-view image into the CCD camera. This plane mirror needs to be finely tuned beforehand to assure the side-view image acquisition.

For the environmental setting in the tongue imaging device, first, in order to reduce the influence of the illumination of where the device is placed, all modules were put inside a nearly closed chest. Only a small acquisition window was left for image acquisition. The dimension of the window was 150×100 mm. Furthermore, to avoid the impact of uneven reflection caused by the interior wall,

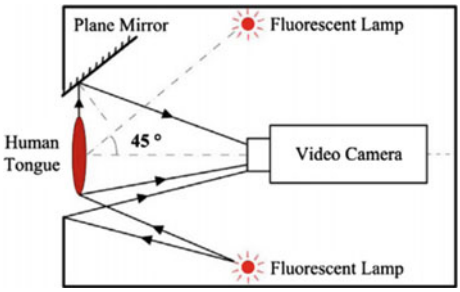

Fig. 2.8 Optical path of the proposed tongue imaging system (*top view*). Reprinted from Wang and Zhang (2013b), with permission from Elsevier

the inside wall was painted with neutral matte grey materials, and thereby the acquired tongue images were robust to illumination variations.

2.3.3 *Imaging Camera*

As Table 2.2 shows, the camera is critical for accurate color and texture rendering. On one hand, its resolution should be high enough to distinguish the smallest texture styles in order to provide images with enough clarity for medical analysis. Additionally, the camera should have a remarkable color rendering capability in order to obtain and classify complex tongue colors. This section will describe how these parameters (resolution and color rendering capability) of an imaging camera were established.

The most important issue for imaging camera selection is to decide what minimum resolution it should have in order to render tongue images with ample clarity. Table 2.1 shows existing utilized cameras with various resolutions, and usually the higher the resolution, the better the tongue texture features. However, the more pixels a tongue image contain, the more computational and storage cost is needed. Thus to discover the minimum resolution for tongue image rendering which is enough to describe the smallest texture feature is essential.

According to oral anatomy (Li, 2011), tongue texture is typically formed by different types of papillae which are microscopic structures on the upper surface of the tongue. As Fig. 2.9 shows, there are four types of papillae presented in a human tongue: filiform, fungiform, foliate, and circumvallate papillae. Among these four kinds of papillae, filiform papillae are the smallest with a dimension around 1–3 mm. Thereby, if the smallest filiform papillae can be distinguished by the imaging camera, all texture styles can be clearly classified.

Suppose the diameter of the smallest filiform papillae is only 1 mm, and there are 3 pixels for each single filiform papilla on average. The resolution would be:

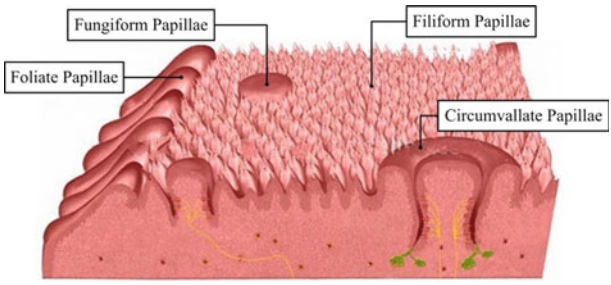

Fig. 2.9 Four types of papillae present in the tongue body which form various kinds of texture types. Reprinted from Wang and Zhang (2013b), with permission from Elsevier

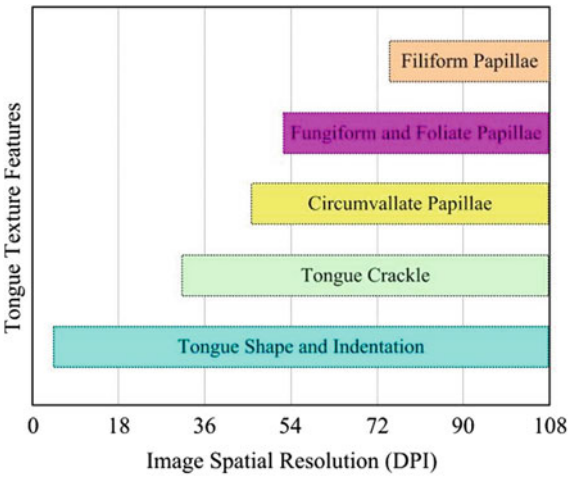

Fig. 2.10 Resolution to ensure sharp tongue texture rendering. The *horizontal axis* represents different imaging resolutions. Each kind of texture can be clearly recorded only when the image resolution reaches the minimum demand. For example, if the image resolution is larger than 30 pixels/in., tongue crackle can be rendered with sufficient clarity. Reprinted from Wang and Zhang (2013b), with permission from Elsevier

$$\text{dpi} = \text{dot/inch} = 3/(1/25.4) \approx 76 \tag{2.2}$$

In the same way, resolution requirements to clearly render other texture styles can also be achieved, and are presented in Fig. 2.10. When the resolution of the chosen imaging camera is larger than the minimum resolution of 76, all texture styles can be clearly quantized for image analysis.

One more consideration for imaging camera selection is to choose a three-CCD (Charge Coupled Device) camera or a single-CCD camera. A three-CCD camera uses three separate CCDs for the measurement of the three primary colors: red, green, and blue. Generally, it can achieve much better precision and provide superior image quality than a single-CCD camera. As tongue color features plays a crucial role in image analysis for medical application, we need to select three-CCD cameras to acquire high quality tongue images.

Another prominent concern of camera selection is to choose a video camera or a still camera. The tongue is an organ which slightly vibrates all the time. Motion blur is usually observed if a digital still camera is used. Therefore, a video camera is more suitable in order to avoid this situation. Also, using a video camera can overcome other drawbacks of still cameras such as unstable illumination and inconsistent exposure degree. Figure 1.8 shows defective images captured by digital still cameras.

According to the above analysis, a three-CCD video camera, Sony DXC 390P, was selected as the tongue imaging camera. This camera is a high-end industrial camera which can acquire 25 images per second. Its spatial resolution is 768 $\times$ 568 pixels. As the size of a human tongue is generally less than 100 $\times$ 80 mm, and the field of view in our system is set to 150 $\times$ 120 mm, the resolution of our system is around 130 pixels/inch, which is large enough to ensure a clear recording of tongue images.

2.3.4 Color Correction

Color images produced by digital cameras suffer from device-dependent color space rendering, i.e., generated color information is dependent on the imaging characteristics of specific cameras. Furthermore, there are usually noises over the color images due to slight variations of the illumination. Therefore, in order to render the color image in a high-quality way, color correction is necessary for accurate image acquisition and is often regarded as a prerequisite before further image analysis.

The color correction process usually involves deriving a transformation between the device-dependent camera RGB values and device-independent color space attributes by the aid of several reference target samples (Munsell colorchecker 24 as Fig. 2.11b shows or tongue colorchecker (Wang & Zhang, 2013a). In our proposed algorithm, the standard RGB (sRGB) color space was chosen as the target device-independent color space because of its distinctive characteristics such as it is commonly used and has a constant relationship with CIELAB to calculate the color difference. Then, as Fig. 2.11a shows, parameters of the correction model were trained by matching color values of the colorchecker from the source device-dependent RGB color space to the device-independent sRGB color space. Finally, this derived correction model was applied on captured tongue images. A polynomial transform-based color correction algorithm was proposed in this system (Wang & Zhang, 2010). The principle of this algorithm is as follows: Suppose that the reference colorchecker has N color patches. For each patch, its quantized color values generated by digital camera can be represented as a vector V: (R_i, G_i, B_i) $(i = 1, 2, \ldots, 24)$, and the corresponding device independent sRGB tri-stimulus values are S: (SR_i, SG_i, SB_i) $(i = 1, 2, \ldots, 24)$. The idea of the polynomial transform based correction algorithm is to map the matrix generated by combining different polynomial terms of the input vector to the objective sRGB vector and thereby obtain the transformation model. For example, if we use the combination of polynomial x: $[R, G, B, 1]$, the transformation model can be represented as follows:

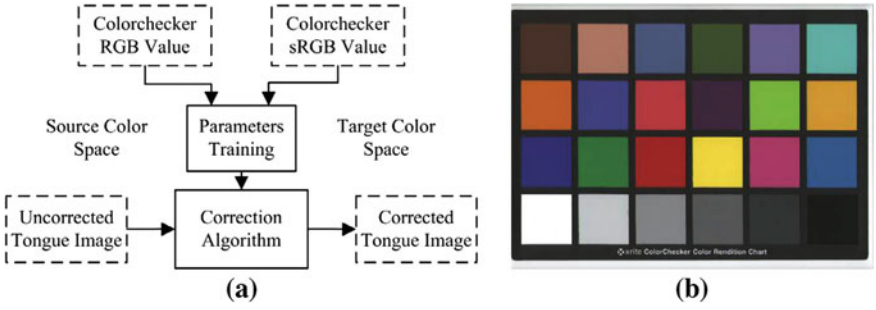

Fig. 2.11 Color correction on tongue images, **a** procedure of the color correction algorithm and **b** Munsell colorchecker 24 was utilized as the reference target for color correction. Reprinted from Wang and Zhang (2013b), with permission from Elsevier

$$\begin{cases} SR_i = a_{11}R_i + a_{12}G_i + a_{13}B_i + a_{14} \\ SG_i = a_{21}R_i + a_{22}G_i + a_{23}B_i + a_{24} \\ SB_i = a_{31}R_i + a_{32}G_i + a_{33}B_i + a_{34} \end{cases} (i = 1, 2, \ldots, 24). \quad (2.3)$$

This equation can also be rewritten in matrix format as

$$\mathbf{S} = \mathbf{A}^{\mathbf{T}} \cdot \mathbf{X} \quad (2.4)$$

where $\boldsymbol{A}$ is the mapping coefficient matrix and $\boldsymbol{X}$ is the matrix generated by different polynomial combinations x. Using the least-square regression method, the solution to (2.4) is as follows:

$$\mathbf{A} = \left(\mathbf{X}^{\mathbf{T}}\mathbf{X}\right)^{-\mathbf{1}}\mathbf{X}^{\mathbf{T}}\mathbf{S} \quad (2.5)$$

We can further apply this transform coefficient matrix $\boldsymbol{A}$ to correct tongue images. Suppose the generated polynomial matrix $\boldsymbol{X}$ for tongue image is $\boldsymbol{X}_{\text{in}}$, then the output image matrix $\boldsymbol{X}_{\text{out}}$ is:

$$\mathbf{X} = \mathbf{A} \cdot \mathbf{X}_{\text{in}} \quad (2.6)$$

By comparing different polynomial combinations which have different numbers of polynomial terms, a polynomial which involves 11 terms x: [R, G, B, RG, RB, GB, R, G_2, B_2, RGB, 1] was employed to train parameters of the correction model based on corresponding attributes of the Munsell colorchecker. This derived correction model was then used on acquired tongue images to render them into a device-independent sRGB color space. Moreover, variations of captured tongue images caused by imaging system components were greatly reduced. Experimental result shows that the CIELAB color difference [calculated as (2.7)] between the estimated values with target ground truth values of the Munsell colorchecker was less than 5 ($\Delta E^*_{ab} < 5$).

$$\Delta E^*_{ab} = \sqrt{\left(L^*_1 - L^*_2\right)^2 + \left(a^*_1 - a^*_2\right)^2 + \left(b^*_1 - b^*_2\right)^2} \quad (2.7)$$

2.3.5 System Implementation and Calibration

As the four core modules were designed in the above sections, this subsection discusses how these modules were implemented together to realize a user-friendly image collection. Also, in order to improve the accuracy and reproducibility of the system, we also illustrate the calibration procedure before it is applied in practice.

In order to make the acquisition procedure user-friendly, several ergonomic concerns have been taken into account. Figure 2.12a shows the appearance of the

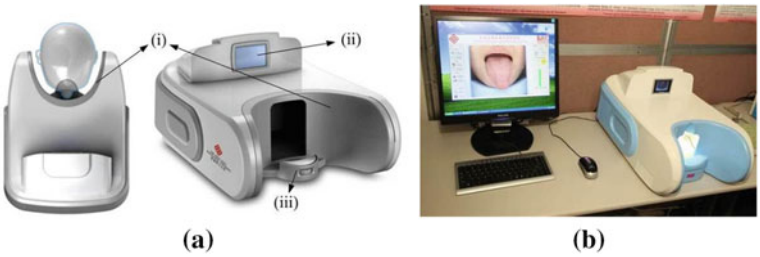

Fig. 2.12 Appearance of the tongue imaging system **a** appearance design and **b** working image of the tongue imaging device. Reprinted from Wang and Zhang (2013b), with permission from Elsevier

tongue imaging system. In order to reduce as much as possible the influence of the environmental illumination, an acquisition interface which perfectly fits the human head model was designed (as (i) in Fig. 2.12a). Furthermore, a small monitor (ii in Fig. 2.12a) was placed at the top of the device to guide users putting their tongue in the appropriate place. Also, a chin rest (iii in Fig. 2.12a) which can hold the user's chin to make them feel comfortable was also added in this device. The working image of this device is shown in Fig. 2.12b. The total dimension of this tongue device is 506 × 370 × 307 mm, and the working distance between the acquisition plane to the camera is 140 mm.

System calibration, which is the process of adjusting a system's accuracy to ensure it is within the designer's specifications, is essential to reduce the measurement uncertainty and improve the quality and consistency of a measurement system. In our system, the system calibration was accomplished through three consecutive steps, which, in sequential order, are the determination of the camera lens aperture, the camera color balance, and the color correction transformation from the device-dependent imaging system space to the device-dependent sRGB space. The aim of all steps is to maximize the accuracy and reproducibility of the imaging system.

2.3.5.1 Camera Lens Aperture

The apertures of a camera lens need to be fixed to avoid overexposure. Usually, it is achieved by setting the camera response to the largest value of 255 for a perfectly reflecting object (white board). In our system, the White Balance ColorChecker (X-rite, Inc., USA) was first imaged by the system, and then, the average value of G channel ($\langle G \rangle$) of a single or a group of pixels in the acquired images was checked. If it was lower than 255, the aperture needed to be enlarged, otherwise, it needed to be narrowed. In sum, the goal is to let the value of the G channel be equal to or close to 255 ($\langle G \rangle = 255$). Actually, to avoid overexposure, this number was set to 254 in practice. This step was executed only one time before the first use of this device, and thereafter this aperture needs to be locked to save the setting. Also, if

possible, this step needs to be re-executed over a period of time (such as 4 weeks or longer) to avoid fluctuation.

2.3.5.2 Camera Color Balance

Usually due to slight variations among the three CCDs, responses of each color channel for a neutral object would be different from others, and this kind of internal systematic error needs to be reduced beforehand. Therefore, the aim of color balance is to ensure that the camera response is equal on its three channels (R, G, and B) for a perfectly neutral object (X-rite Gray Balance ColorChecker in this system). In a real case, the gray colorchecker is first imaged, and then, the offset for each channel is adjusted to ensure $(R) = (G) = (B)$. In our proposed system, the imaging camera was equipped with a 10-bit digital signal processor (DSP), and thus this offset adjustment could be directly conducted and saved. This procedure only needs to be executed once before the first use of this device, but it needs to be re-checked at regular intervals.

2.3.5.3 Color Correction Model

The proposed polynomial-based color correction algorithm was implemented into the built-in embedded system to correct every tongue image before it is saved into the database. The correction procedure is as follows. First, the Munsell colorchecker 24 was imaged by the camera to get the colorchecker image, then the 24 color values of these colorchecker image were automatically extracted by our implemented extraction program. This program can automatically extract the average value for each color patch. Finally, the color correction matrix was obtained by mapping these extracted 24 color values to their standard values (color attributed in sRGB colors space). This derived correction model was saved in the embedded system and applied for correction of all acquired tongue images in the same session. Also, it is only valid for one session and needs to be executed every time before the system is rebooted or reused.

2.4 Performance Analysis

The proposed system was tested in terms of three aspects: illumination uniformity, accuracy which measures the quality of the acquired image, and consistency which measures the precision or reproducibility among different capture sessions or different devices. These performance analysis results are presented as follows.

2.4.1 Illumination Uniformity

Illumination uniformity, which is used to measure the relationship of the spatial distribution of illuminance across the working area, is important for high-quality image rendering (Rea, 2000). Poor uniformity, especially shadows, may distort the visual perception of objects. Based on the statistical analysis of the distribution of illumination, there are several definitions that express uniformity, and the most common one is the min–max ratio (U_1):

$$U_1 = E_{\min}/E_{\max} \tag{2.8}$$

where $E_{\min}$ and $E_{\max}$ are the minimum and maximum illuminance. Another popular one is the contrast ratio: $U_2 = (E_{\max} - E_{\min})/(E_{\max} + E_{\min})$. Additionally, several metrics based on statistics were also proposed, such as the minimum-average ratio: $U_3 = E_{\min}/\overline{E} = E_{\min}\left(\sum_{i=1}^{N} E_i/N\right)^{-1}$, and the ratio of the standard deviation to the mean (also known as coefficient of variation):

$$\mathrm{CV} = \sigma_E/\overline{E} = \left[\sum_{i=1}^{N}\left(E_i/\overline{E} - 1\right)^2/(N-1)\right]^{0.5} \tag{2.9}$$

where $\overline{E}$ and σ_E are the mean and standard deviation of the illuminance respectively.

In this experiment, the Munsell gray colorchecker was first imaged by the designed device, and then, intensity values of all pixels in this image were used to calculate the uniformity of illumination. Based on the above calculation formulas, the uniformity of our proposed imaging system was obtained as Table 2.3 shows. From this table, it can be seen that the min–max ratio was 0.8617. Compared to the minimum uniformity of the standard illumination condition recommended by ISO 3664 which is 0.75, this result shows that the uniformity in our system is much better than recommended the ISO standard. Moreover, the measurement of CV shows that the illuminant slightly changes across the acquisition plane because the standard deviation σ_E is very small. In sum, these results show that the developed device provides a uniform illuminance condition for tongue image acquisition.

Table 2.3 Illumination uniformity of the proposed imaging system

	U_1	U_2	U_3	CV
Uniformity	0.867	0.0743	0.9135	0.0641
Reference value	0.75			

Reprinted from Wang and Zhang (2013b), with permission from Elsevier

2.4.2 System Consistency

Consistency is the precision or the reproducibility of measurement, or the degree of repeated measurements that is close to the average of those measurements which are conducted under different conditions, such as at different time points, in different locations or by different imaging devices. According to various measurements conditions, different types of consistency can be distinguished: consecutive consistency (σ_1), intra-run consistency (σ_2), inter-run consistency (σ_3), and between-device consistency (σ_4). Consistency testing experiments are normally conducted based on a reference target such as a colorchecker which has fixed number of color patches. In this experiment, the Munsell colorchecker 24 (Mccamy, Marcus, & Davidson, 1976; X-Rite, 2012), which is regarded as the de facto standard for visual evaluation, was utilized as the reference object because of its popular usage. It was imaged many times under different conditions. Then, in order to quantitatively calculate the degree of consistency, the average CIE color difference between these 24 color values of the colorchecker was calculated according to (2.7).

Figure 2.13 shows an illustration of these four types of consistency. The consecutive consistency (σ_1) computes the average color difference among five images continuously acquitted within a short time interval (less than 10 s) at a specific time point. This metric describes the minimum difference produced by this device, and it thus can be regarded as a benchmark for the consistency measurement. The intra-run consistency (σ_2), also named as within-run consistency or precision, measures the difference among images acquired at different time points within a single acquisition session. In this experiment, images were captured at 6 different time points, i.e., 0, 1, 2, 3, 5, and 10 min after the system was started. A system needs to be stabilized before it can be applied in practice. Therefore, by computing the color difference among these 6 images, we could not only obtain the value of intra-run consistency but also find how long of this system needed to become stable. Also, by this measurement, we can also evaluate the influence of temperature

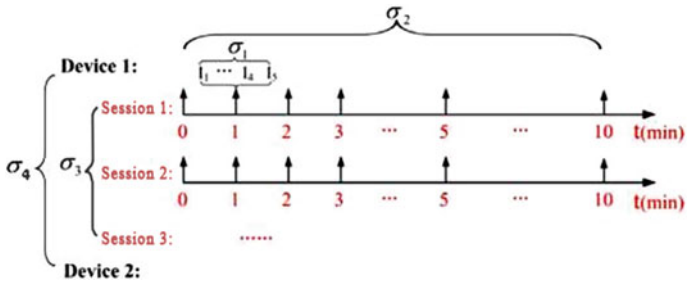

Fig. 2.13 Four kinds of consistency measurements, i.e., consecutive consistency (σ_1), intra-run consistency (σ_2), inter-run consistency (σ_3), and between-device consistency (σ_4). These four metrics are designed to describe the reproducibility of the imaging system

Table 2.4 Experimental result of consecutive consistency σ_1

Time point	t1	t2	t3	t4	t5	t6
Average $\Delta E^*_{ab} < 5$	0.5485	0.5886	0.4708	0.4365	0.4872	0.4343

Reprinted from Wang and Zhang (2013b), with permission from Elsevier

variation when the system works. The inter-run consistency (σ_3), also named as between-run consistency, measures the degree of closeness among images captured from different capture session with the same imaging device. In order to test the repeatability of the system, especially the time durability, we captured three sessions of the Munsell colorchecker. The first session was captured after the system was just implemented (a brand-new system). Session 2 was conducted half a month after session 1, and images from session 3 were taken one year after the time of session 1. Finally, the between-device consistency (σ_4), shows the degree of reproducibility between two acquisition devices which have the same components and configuration.

2.4.2.1 Consecutive Consistency

Table 2.4 presents the results of consecutive consistency (σ_1) in session 1. We captured 5 images at each time point (t1–t6), and calculated the average color difference among them by first adding the color difference of all 24 color patches and then dividing by 24. From Table 2.4, it can be seen that σ_1 was around 0.4343–0.5886. At the beginning, after the device just started (t1 and t2), the color difference between continuously acquired tongue images was bigger than 0.5485. Then, when the device is stable, this number decreased and stabilized around 0.48. This result also shows that the minimum color difference produced by this developed imaging system was less than 0.5, which is almost indistinguishable by the human eye.

2.4.2.2 Intra-run Consistency

For the intra-run consistency (σ_2), the color difference among images from session 1 was calculated as an example. Also, in order to explore the main cause which leads to this kind of intra-run variation, the intensity difference between images captured from consecutive time points was also calculated to find if these two kinds of differences are correlated. In this experiment, the intensity difference between two colorchecker was obtained by calculating the absolute value of the lightness difference for the same neutral patch. We transferred the image from RGB color space to CIE LAB color space, and the difference on the L component represents the intensity difference. From Table 2.5, it can be seen that both the average color difference and intensity difference gradually decrease, i.e., from 2.6934 to 0.5331 and 3.4247 to 0.5141 respectively. What is more, the same decreasing trend can be

Table 2.5 Experimental result of the intra-run consistency (σ_2)

	t2–t1	t3–t2	t4–t3	t5–t4	t6–t5
Average $\Delta E^*_{ab} < 5$	2.6934	0.7294	0.5465	0.5597	0.5331
Intensity difference	3.4247	0.3316	0.4314	0.3344	0.5141
Correlation coefficient	0.9918				

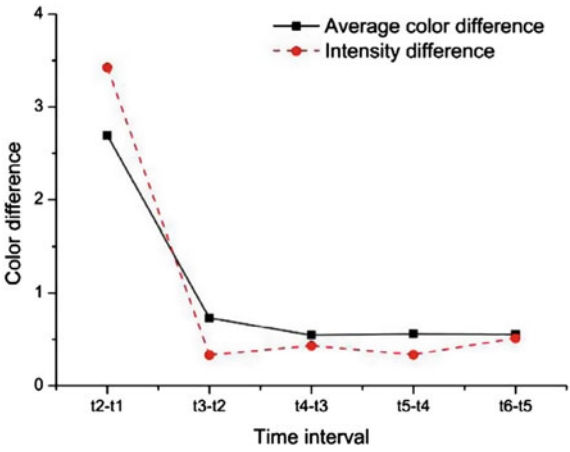

Fig. 2.14 Results of intra-run consistency. The color difference and intensity difference present a similar decreasing trend which illustrates they are highly correlated with each other. Reprinted from Wang and Zhang (2013b), with permission from Elsevier

noticed from Fig. 2.14. Values of color difference dropped dramatically during the first 1–2 min, and then they became stable at a specific level. Moreover, the result of the correlation coefficient which was 0.9918 also illustrates they are highly correlated with each other. From these results, the three findings can be summarized. First, the system needs to be stabilized before real acquisition, and this stabilization usually requires 1–2 min. Second, the intra-run consistency is around 0.55. Although it is larger than the consecutive consistency of 0.48, this color difference is still small enough to be ignored. Third, this kind of intra-run difference is possibly caused by the instability of illumination because the average color difference is highly correlated to the intensity variation (the correlation coefficient is 0.9918).

2.4.2.3 Inter-run Consistency

The inter-run consistency describes the closeness of images captured at different capture sessions. Ordinarily a session here means the time span between the system startup and shutdown. We captured images at three separate sessions after the system was completely stabilized. Session 1 was captured by a brand-new device, session 2 was obtained by the same device half a month later, while session 3 was nearly one year later. The same as for the analysis of intra-run consistency, both the

Table 2.6 Experimental result of the inter-run consistency (r3) among three separate sessions

	(s1, s2)	(s2, s3)	(s1, s3)
Average $\Delta E^*_{ab} < 5$	0.5034	0.5436	0.6389
Intensity difference	0.3956	0.5742	0.6698
Correlation coefficient	0.9196		

Reprinted from Wang and Zhang (2013b), with permission from Elsevier

average color difference and intensity difference are provided in Table 2.6. In this table, (s1, s2) represents the difference between images captured in session 1 and session 2. Surprisingly, it may be noted that the inter-run precision is almost of the same order of magnitude as the intra-run consistency, which is between 0.5034 and 0.6389. This result shows that the system is fairly stable in achieving high-consistent tongue image acquisition. Regarding the time durability, we found that there was no substantial difference among images captured at different times. Despite the fact that the (s1, s3) difference is larger than the other two cases, it is still very small and cannot be noticed by human inspection. This result shows that the device can retain high quality for a very long time. Also, if possible, more experiments need to be conducted to test color difference for a longer time such as two years or five years. The same as for the result of intra-run consistency, we found that this between-run difference is also closely related to intensity difference caused by the fluctuation of illumination because their correlation coefficient is 0.9405.

2.4.2.4 Between-Device Consistency

The above results show that a single well-calibrated imaging device can achieve highly consistent tongue image acquisition. Furthermore, the consistency among different devices which have the same imaging components and configuration, i.e., between-device precision or batch reproducibility, is also crucial for system performance. We developed two imaging systems according to our proposed specification. After calibration, these two devices were supposed to have the same image rendering ability. In this experiment, the same Munsell colorchecker 24 was first imaged by these two devices, and then the color difference was calculated to measure the between-device precision. We captured 5 groups of images for each of these two devices, and calculated color differences between them which are shown in Table 2.7. The results show that the difference between these two devices was between 1.0341 and 1.6532. Obviously, the between-device precision is larger than

Table 2.7 Experimental result of the between-device consistency (σ_4)

Group no.	1	2	3	4	5
Average $\Delta E^*_{ab} < 5$	1.2038	1.6532	1.5982	1.0341	1.3647

Reprinted from Wang and Zhang (2013b), with permission from Elsevier

its inter-device counterpart (including inter-run and intra-run consistency) which is around 0.5. A possible explanation for why the between-device variation is much larger is as follows. The inter-device variation is principally generated because of the fluctuation of illumination which belongs to random error, and this kind of random error cannot be completely eliminated. Moreover, in addition to the random error, another factor which makes the two devices different is the variance of imaging characteristic of the camera. Regardless of the fact that the calibration procedure may reduce this kind of disparity, it belongs to systematic error and cannot be fully eliminated.

2.4.3 Accuracy

Accuracy is the way in which the measurement made by the imaging system is close to its true value which is usually measured by other reference instruments. In this experiment, as the texture information is usually easily acquired in high fidelity, a test on accuracy of chromatic feature rendering was the main objective.

To quantify the accuracy of this imaging system, we computed the average and maximal CIE color difference $\Delta E^*_{ab} < 5$ over a test colorchecker, i.e., the Munsell colorchecker 24. Several colors of this chart were used as a reference target for model training in system calibration. We captured five images of this test colorchecker at different times when the system was stabilized. Table 2.8 shows the results of the accuracy test. It shows that the average color difference between the acquired image when its true value is smaller than 4, is unnoticeable to the human eye. Also, the maximum and minimum color differences show that variations among these 24 tested colors are minor, which illustrates that the imaging system can accurately render all colors.

2.4.4 Typical Tongue Images

The developed tongue imaging system has been utilized in practical image acquisition in a hospital for almost 3 years. Doctors of Traditional Chinese Medicine have also thoroughly evaluated this device during real applications. To date, a large and comprehensive tongue image database has been established. This database includes over 9000 images which were collected from 5222 subjects, in which over

Table 2.8 Accuracy test of the proposed imaging device

Test image no.	Average $\Delta E^*_{ab} < 5$	Max. $\Delta E^*_{ab} < 5$	Min. $\Delta E^*_{ab} < 5$
1	3.9079	8.1551	0.7959
2	3.8652	7.7201	1.1914
3	3.7873	8.2872	1.1385

Reprinted from Wang and Zhang (2013b), with permission from Elsevier

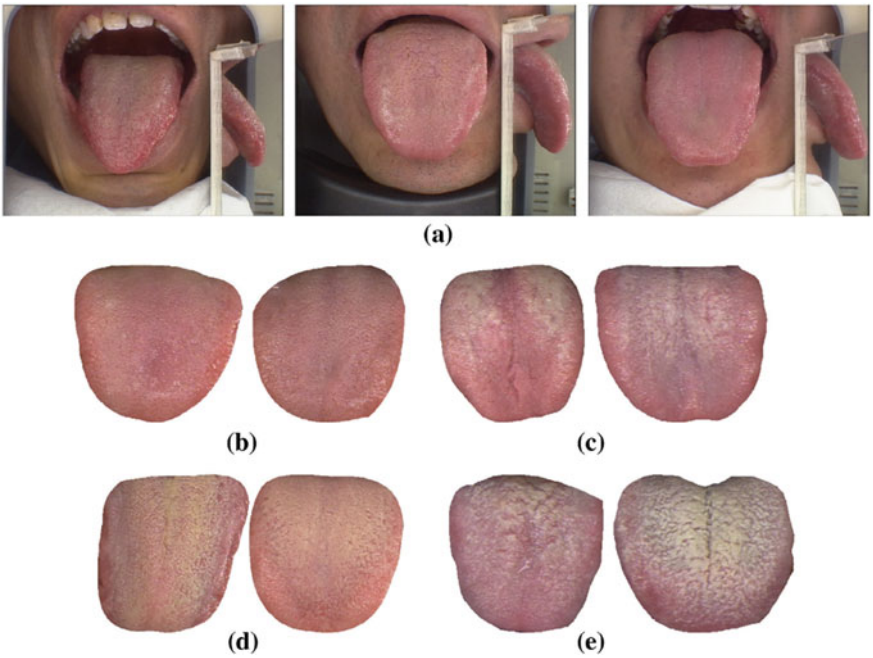

Fig. 2.15 Typical tongue images acquired by our proposed imaging system. **a** Shows three original images which contain side-view images. Other images are the pure tongue body which was extracted from background. They are in different health statuses, including: **b** healthy, **c** pneumonia, **d** chronic kidney disease, and **e** pancreatitis. The proposed system can faithfully render all kinds of colors, textures, and geometric features. Reprinted from Wang and Zhang (2013b), with permission from Elsevier

2780 subjects were patients in almost 200 disease types. Several typical images acquired by this developed system are shown in Fig. 2.15. Obviously, images with different health statuses have different chromatic and texture characteristics. For example, images from people with appendicitis (Fig. 2.15b) are commonly a deep red color and have a lot of red-points, and images from people with chronic kidney disease contain a lot of yellow color components. These obtained images have been applied to medical analysis of disease diagnosis, and preliminary results verify the effectiveness of this system. Furthermore, we are also planning to open this database to other researchers for academic usage in the future.

2.5 Summary

This chapter conducted a thorough and fundamental study on the development of an accurate and consistent tongue imaging device for computerized tongue image analysis. There are mainly two contributions of this study. First, a series of

guidelines for a tongue imaging system design were presented. This is the first proposed design guideline in the research community, and it can even be regarded as a design standard because most of the proposed criteria were constructed by international standards on color imaging technology. Second, a new tongue imaging system was presented in this work, and several components were first designed in this system, such as the plane mirror to capture the side-view image, the embedded system to enhance the mobility, and the minimum resolution of a CCD camera for tongue imaging.

Compared to existing devices, this proposed system is more accurate and stable. By following the guideline, all system components have been optimally designed, and hence all possible medical clues including the tongue width can be acquired by this device in high quality. Moreover, with the help of the implemented embedded system, this device is more convenient and portable. This would grant the system a wider and deeper utilization in real computerized tongue diagnosis applications. Unlike other existing devices, this developed system was completely tested for its accuracy and consistency before it was applied in practice. Test results show that captured images remain stable when acquisition is repeated at different time points or by different devices. The biggest observed color difference ($\Delta E^*_{ab} < 5$) between two images acquired by two devices is 1.6532, which is hard to be distinguished by the human eye. Besides these kinds of performance evaluation, the proposed system has been utilized to capture over 9000 tongue images in the hospital, and preliminary analysis results also validate the effectiveness and advantages of this system.

Theoretically speaking, all elements in this device have been optimally designed, and an implemented device following these design criteria should have similar high quality.

References

Cai, Y. (2002). A novel imaging system for tongue inspection (pp. 159–164). IEEE, 1999.

Chiu, C. (2000). A novel approach based on computerized image analysis for traditional Chinese medical diagnosis of the tongue. *Computer Methods and Programs in Biomedicine, 61*(2), 77–89.

Du, H., Liu, Z., Li, Q., Yan, J., & Tang, Q. (2007). A novel hyperspectral medical sensor for tongue diagnosis. *Sensor Review, 27*(1), 57–60.

He, Y., Liu, C., & Shen, L. (2007). Digital camera based tongue manifestation acquisition platform. *World Science and Technology-Modernization of Traditional Chinese Medicine and Materia Medica, 5*.

Huang, B., Wu, J., Zhang, D., & Li, N. (2010). Tongue shape classification by geometric features. *Information Sciences, 180*(2), 312–324.

ISO. (2009). Graphic technology and photography—Viewing conditions.

Jang, J. H., Kim, J. E., Park, K. M., Park, S. O., Chang, Y. S., & Kim, B. Y. (2002). Development of the digital tongue inspection system with image analysis (pp. 1033–1034). IEEE.

Jiang, Y. W., Chen, J. Z., & Zhang, H. H. (2000). Computerized system of diagnosis of tongue in Traditional Chinese Medicine. *Chinese Journal of Integrated Traditional and Western Medicine, 20*(2), 145–147.

Li, N. (2011). *Tongue diagnostics*. Cambridge: Academy Press.

Li, Q., & Liu, Z. (2009). Tongue color analysis and discrimination based on hyperspectral images. *Computerized Medical Imaging and Graphics, 33*(3), 217–221.

Li, Q., Wang, Y., Liu, H., & Sun, Z. (2010). AOTF based hyperspectral tongue imaging system and its applications in computer-aided tongue disease diagnosis (pp. 1424–1427).

Li, Q., Wang, Y., Liu, H., Sun, Z., & Liu, Z. (2010b). Tongue fissure extraction and classification using hyperspectral imaging technology. *Applied Optics, 49*(11), 2006–2013.

Maciocia, G. (1987). *Tongue diagnosis in Chinese medicine*. Seattle: Eastland Press.

Maciocia, G. (2013). *Diagnosis in Chinese medicine: A comprehensive guide*. Amsterdam: Elsevier Health Sciences.

Mccamy, C. S., Marcus, H., & Davidson, J. G. (1976). A color-rendition Chart. *Journal of Applied Photographic Engineering, 2*, 95–99.

Pang, B., Zhang, D., Li, N., & Wang, K. 2004. Computerized tongue diagnosis based on Bayesian networks. *IEEE Transactions on Biomedical Engineering, 51*(10), 1803–1810.

Rea, B. M., & Ed. (2000). *Iesna lighting handbook* (9th ed.). Illuminating engineering society of north america.

Wang, X., & Zhang, D. (2010). An optimized tongue image color correction scheme. *IEEE Transactions on Information Technology in Biomedicine, 14*(6), 1355–1364.

Wang, X., & Zhang, D. (2013a). A new tongue colorchecker design by space representation for precise correction. *IEEE Journal of Biomedical and Health Informatics, 17*(2), 381–391.

Wang, X., & Zhang, D. (2013b). A high quality color imaging system for computerized tongue image analysis. *Expert Systems with Applications*, *40*(15), 5854–5866.

Wang, Y., Zhou, Y., Yang, J., & Xu, Q. (2004). An image analysis system for tongue diagnosis in traditional Chinese medicine. In *Computational and information science* (pp. 1181–1186). Berlin: Springer.

Wei, B. G., Shen, L. S., Wang, Y. Q., Wang, Y. G., Wang, A. M. & Zhao, Z. X. (2002). A digital tongue image analysis instrument for Traditional Chinese Medicine. *Chinese Journal of Medical Instrumentation* [*Zhongguo yi liao qi xie za zhi*], *26*(3), 164–166.

Wong, W., & Huang, S. (2001). Studies on externalization of application of tongue inspection of TCM. *Engineering Science, 3*(1), 78–82.

X-Rite. (2012). Munsell ColorChecker Classic.

Zhang, H. Z., Wang, K. Q., Zhang, D., Pang, B., & Huang, B. (2005). *Computer aided tongue diagnosis system* (pp. 6754–6757). IEEE.

http://www.springer.com/978-981-10-2166-4

Tongue Image Analysis

Zhang, D.; Zhang, H.; Zhang, B.

2017, XV, 335 p. 193 illus., 144 illus. in color.,
Hardcover
ISBN: 978-981-10-2166-4